

Wave Modes in the Magnetospheres of Pulsars and Magnetars

Chen Wang^{1,2} and Dong Lai^{2,1}

¹*National Astronomical Observatories, Chinese Academy of Sciences. A20 Datun Road, Chaoyang District, Beijing 100012, China*

²*Center for Radiophysics and Space Research, Department of Astronomy, Cornell University. Ithaca, NY 14853, USA*

E-mail: wangchen@bao.ac.cn, dong@astro.cornell.edu

Accepted 2006 xxx, Received 2006 xxx; in original form 2006 xxx

ABSTRACT

We study the wave propagation modes in the relativistic streaming pair plasma of the magnetospheres of pulsars and magnetars, focusing on the effect of vacuum polarization. We show that the combined plasma and vacuum polarization effects give rise to a vacuum resonance, where “avoided mode crossing” occurs between the extraordinary mode and the (superluminous) ordinary mode. When a photon propagates from the vacuum-polarization-dominated region at small radii to the plasma-dominated region at large radii, its polarization state may undergo significant change across the vacuum resonance. We map out the parameter regimes (e.g., field strength, plasma density and Lorentz factor) under which the vacuum resonance occurs and examine how wave propagation is affected by the resonance. Some possible applications of our results are discussed, including high-frequency radio emission from pulsars and possibly magnetars, and optical/IR emission from neutron star surfaces and inner magnetospheres.

Key words: plasmas – polarization – waves – star: magnetic fields – pulsars: general

1 INTRODUCTION

The magnetospheres of pulsars and magnetars consist of relativistic electron-positron pair plasmas, plus possibly a small amount of ions. These plasmas can affect the radiation produced in the inner region of the magnetosphere or the stellar surface. Understanding the property of wave propagation in pulsar/magnetar magnetospheres is important for the interpretation of various observations of these objects.

Radio emission from pulsars (at least “normal” – non millisecond – pulsars) likely originates from close to the stellar surface, within a few percent of light cylinder radius (e.g., Blaskiewicz et al. 1991, Kramer et al. 1997). A number of studies have been devoted to the propagation effect of radio waves in pulsar magnetospheres (e.g., Cheng & Ruderman 1979; Barnard & Arons 1986; Barnard 1986; Lyubarskii & Petrova 1998; Melrose & Luo 2004; Petrova 2006). Some of the observed polarization properties of pulsar emission, such as orthogonal modes (in which the polarization position angle exhibits a sudden $\sim 90^\circ$ jumps; e.g. Stinebring et al. 1984a, 1984b) and circular polarization (e.g., Radhakrishnan & Rankin 1990; Han et al. 1998; You & Han 2006) may be explained by the propagation effect. In addition, optical/IR radiation may be produced in the inner magnetosphere or surface of magnetized neutron stars. For example, while for most radio pulsars the optical and near IR flux is thought to be dominated by magnetospheric emission, several middle-aged pulsars (PSR B0656+14, PSR B0950+08 and Geminga) also exhibit a surface optical component (e.g., Mignani, de Luca & Caraveo 2004; Kargaltsev et al. 2005, Mignani et al. 2006). The optical emission detected in several thermally emitting, isolated neutron stars mostly likely has a surface origin (e.g., Kaplan et al. 2003; Haberl et al. 2004; Haberl 2005; van KerKwijk & Kaplan 2006). Finally, the optical/IR emission detected from a number of magnetars may originate from a hot corona near the stellar surface (Beloborodov & Thompson 2006).

Wave modes in pulsar magnetospheres have been studied in a number of papers under different assumptions about the plasma composition and the velocity distribution of electron-positron pairs (e.g., Melrose & Stoneham 1977; Arons & Barnard 1986; Lyutikov 1998; Melrose et al. 1999; Asseo & Riazuelo 2000). In this paper, we reinvestigate the property of wave propagation in the magnetospheres of pulsars and magnetars, focusing on the competition between the plasma effect and the effect of vacuum polarization. It is well known that in the strong magnetic field typically found on a neutron star,

the electromagnetic dispersion relation is dominated by vacuum polarization (a prediction of quantum electrodynamics; e.g., Heisenberg & Euler 1936; Adler 1971; see Schubert 2000 for extensive bibliography) at high photon frequencies (e.g. X-rays) and by the plasma effect at sufficiently low frequencies (e.g., radio waves). But where is the “boundary” at which the two effects are “equal” and what are the mode proportion in the “boundary” regime? These are the questions we are trying to address in this paper. We show that the combined plasma and vacuum polarization effects give rise to a *vacuum resonance*: For a given plasma parameters and external magnetic field, there exists a special photon frequency at which the plasma effect and vacuum polarization effects “cancel” each other. A more physical way to describe the resonance is as follows: Consider a photon propagating in the inhomogeneous pulsar/magnetar magnetosphere with varying plasma density (and/or distribution function) and magnetic field. For certain parameter regimes of the photon frequency, plasma density and magnetic field strength — to be determined in the following sections, the photon may traverse from the vacuum-polarization-dominated region to the plasma-dominated region or vice versa. This transition point (location) is the vacuum resonance. When the photon crosses this resonance, its polarization state may undergo significant change. The goal of our paper is to map out the parameter regimes under which the vacuum resonance may occur and to elucidate how wave propagation may be affected by the resonance.

Vacuum resonance in cold, non-streaming plasmas have been studied before (e.g., Gnedin et al. 1978; Mészáros & Veutura 1979; Lai & Ho 2002, 2003a). In the atmospheres of highly magnetized neutron stars, the resonance can significantly affect the surface emission spectrum and polarization (Ho & Lai 2003; Lai & Ho 2003a, b; van Adelsberg & Lai 2006). We note that while some previous papers on wave modes in pulsar magnetospheres (e.g. Arons & Barnard 1986) did include the vacuum polarization contributions to the dielectric tensor, the vacuum resonance phenomenon was neglected because it is unimportant at the low frequencies and magnetic fields they considered.

Our paper is organized as follows. In §2, we give the expression for the dielectric tensor of a relativistic pair plasma characterizing the magnetosphere of pulsars/magnetars, including the contribution due to vacuum polarization. In §3, we derive the general expression for wave modes in the combined “plasma + vacuum” medium, and show that the vacuum resonance arises for a wide range of magnetosphere parameters. In §4 we study the evolution of wave mode across the vacuum resonance. In most of this paper, we consider cold, streaming plasma with a single Lorentz factor γ . We examine the effect of a more general γ distribution in §5 and the case of opposite plasma streams in §6. In §7 we discuss possible applications of our results.

2 DIELECTRIC TENSOR FOR AN STREAMING ELECTRON-POSITRON PLASMA

We consider an electron-positron plasma in the magnetosphere of a neutron star (NS). Let N_- , N_+ be the number densities of electrons and positrons, respectively, $N = N_- + N_+$ the total density, and $f = N_+/N$ the positron fraction. The corotation region of the magnetosphere is usually assumed to have Goldreich-Julian charge density

$$\rho_e = -\frac{1}{2\pi c}\boldsymbol{\Omega} \cdot \mathbf{B}, \quad (2.1)$$

where $\boldsymbol{\Omega}$ is the angular velocity of the star. This is not necessarily the case in the open-field line region. In this paper we shall use the Goldreich-Julian number density as a fiducial value:

$$N_{\text{GJ}} = \frac{\Omega B}{2\pi e c} \simeq 7.0 \times 10^{10} B_{12} P_1^{-1} \text{ cm}^{-3}. \quad (2.2)$$

where $B_{12} = B/(10^{12} \text{ G})$, P_1 is the spin period in units of 1 s. The actual particle density N is larger than N_{GJ} by a factor of η , i.e. $N = \eta N_{\text{GJ}}$, with $\eta \geq 1$. If the charge density is equal to the Goldreich-Julian value, then $\eta(1 - 2f) = 1$, but we will not entirely restrict ourselves to this constraint.

Although the plasma is expected to be relativistic, it is useful to define the (nonrelativistic) cyclotron frequencies and plasma frequencies of electron and positron:

$$\omega_c = \omega_{c+} = \omega_{c-} = \frac{eB}{m_e c}, \quad (2.3)$$

$$\omega_{p-}^2 = \frac{4\pi N_- e^2}{m_e} = (1 - f)\omega_p^2, \quad (2.4)$$

$$\omega_{p+}^2 = \frac{4\pi N_+ e^2}{m_e} = f\omega_p^2, \quad (2.5)$$

$$\omega_p^2 = \frac{4\pi N e^2}{m_e}. \quad (2.6)$$

The characteristic values are

$$\nu_c = \frac{\omega_c}{2\pi} = 2.795 \times 10^9 B_{12} \text{ GHz} \quad (2.7)$$

$$\nu_p = \frac{\omega_p}{2\pi} = 8.960 \times 10^3 N^{1/2} \text{ Hz} = 2.370 \eta^{1/2} B_{12}^{1/2} P_1^{-1/2} \text{ GHz}, \quad (2.8)$$

Because of the very short cyclotron/synchrotron decay time of electrons and positrons ($\approx 3 \times 10^{-16} B_{12}^{-2} \gamma \text{ sec}$), all the particles in the magnetosphere quickly lose their transverse momenta and stay in the lowest Landau level. Thus the magnetosphere pair plasma can be considered as one-dimensional, with the particles streaming along the field line. The Lorentz factor γ of the streaming motion is uncertain. In the polar-cap region of a pulsar, primary particles may be accelerated to very high energy ($\gamma \sim 10^6 - 10^7$) by a field-aligned electric field. The bulk of the plasma produced in an electromagnetic cascade may have lower energies, $\gamma \sim 10^2 - 10^4$, with multiplicity factor $\eta \sim 10^2 - 10^5$ (e.g., Dangherty & Harding 1982; Hibschan & Arons 2001). Kunzl et al. (1998) argued that too high a density of secondary particles in the magnetosphere is in contradiction to the observed low-frequency emission from radio pulsars, implying $\eta \lesssim 100$. The physical parameters for the plasma in the closed-field-line region of a pulsar are also not well constrained. It was suggested that a pair plasma density larger than N_{GJ} may be present, maintained by conversion of γ -rays from the pulsar's polar-cap and/or out-gap accelerators (see Wang et al. 1998; Ruderman 2003).

For magnetars, recent theoretical work suggests that a corona consisting mainly of relativistic pairs with $\gamma \sim 10^3$ (and a wide spread in γ) may be generated by crustal magnetic field twisting/shearing due to starquakes (Thompson et al. 2002; Beloborodov & Thompson 2006). The plasma density is of order $N \sim |\nabla \times \mathbf{B}|/(4\pi e) \sim B/(4\pi e r)$ (for a twist angle of order unity), implying $\eta = N/N_{GJ} \sim c/(2\Omega r) \simeq 2 \times 10^3 (R/r)$ (where R is the stellar radius). There are roughly equal amount of electrons and positrons, $f \simeq 1/2$, with the electrons and positrons streams in opposite directions.

2.1 Cold, Streaming Pair Plasma

We first consider a cold electron-positron plasma with all the electron streaming with velocity $\mathbf{V}_{-,0}$ and positron all with $\mathbf{V}_{+,0}$ which is also along the magnetic field \mathbf{B}_0 . The dielectric tensor for such a plasma was derived by Melrose & Stoneham (1977) based on Lorentz transformation (see also Melrose 1973). Here we outline a derivation based on classical magneto-ionic theory.

The equation of motion of a given charge species (mass $m_s = m_e$, charge $q_s = \pm e$, $s = \pm$) reads

$$\frac{d}{dt} (\gamma_s m_s \mathbf{V}_s) = q_s \mathbf{E} + \frac{q_s}{c} \mathbf{V}_s \times \mathbf{B}, \quad (2.9)$$

where $\beta_s = V_s/c$, $\gamma_s = (1 - V_s^2/c^2)^{-1/2}$, $\mathbf{V}_s = \mathbf{V}_{s,0} + \delta \mathbf{V}_s$, $\mathbf{E} = \delta \mathbf{E}$, $\mathbf{B} = \mathbf{B}_0 + \delta \mathbf{B}$. Here $\delta \mathbf{V}_s$, $\delta \mathbf{E}$, $\delta \mathbf{B}$ are associated with the disturbance in the plasma, and have the form $e^{i(\mathbf{k} \cdot \mathbf{r} - \omega t)}$. With $d\delta \mathbf{V}_s/dt = -i\omega \delta \mathbf{V}_s + ic(\mathbf{k} \cdot \mathbf{V}_{s,0}) \delta \mathbf{V}_s$ and $\delta \mathbf{B} = (c\mathbf{k}/\omega) \times \delta \mathbf{E}$, we can solve for $\delta \mathbf{V}_s$ in terms of the components of $\delta \mathbf{E}$. The current density associated with the disturbance is

$$\delta \mathbf{J} = \sum_s (N_s q_s \delta \mathbf{V}_s + \delta N_s q_s \mathbf{V}_{s,0}), \quad (2.10)$$

where the sum runs over each charged particle species s (electron e and positron p). The density perturbation δN_s is determined by the continuity equation, $\partial N_s / \partial t = -\nabla \cdot (N_s \mathbf{V}_{s,0})$, which gives $\delta N_s = N_s (\mathbf{k} \cdot \delta \mathbf{V}_s) / (\omega - \mathbf{k} \cdot \mathbf{V}_{s,0})$. The conductivity tensor is defined by $\delta \mathbf{J} = \boldsymbol{\sigma} \cdot \delta \mathbf{E}$, and the dielectric tensor is given by $\boldsymbol{\epsilon} = \mathbf{I} + i(4\pi c/\omega) \boldsymbol{\sigma}$, where \mathbf{I} is the unit tensor. In the coordinate system $x'y'z'$ with $\hat{\mathbf{B}}_0/|\mathbf{B}_0|$ along \mathbf{z}' , and \mathbf{k} in the $\mathbf{x}'\text{-}\mathbf{z}'$ plane, such that $\hat{\mathbf{k}} \times \hat{\mathbf{B}}_0 = -\sin \theta_B \hat{\mathbf{y}}'$ (θ_B is the angle between $\hat{\mathbf{k}}$ and $\hat{\mathbf{B}}_0$), we find

$$\boldsymbol{\epsilon}^{(p)} = \begin{bmatrix} S & iD & A \\ -iD & S & -iC \\ A & iC & P \end{bmatrix}, \quad (2.11)$$

with

$$\begin{aligned} S &= 1 + \sum_s f_{s,11}, \\ D &= \sum_s f_{s,12}, \\ A &= \sum_s \zeta_s f_{s,11}, \\ C &= \sum_s \zeta_s f_{s,12}, \\ P &= 1 + \sum_s (f_{s,\eta} + \zeta_s^2 f_{s,11}), \end{aligned} \quad (2.12)$$

where

$$\begin{aligned}
f_{s,11} &= -\frac{v_s \gamma_s^{-1}}{1 - u_s \gamma_s^{-2} (1 - n \beta_s \cos \theta_B)^{-2}}, \\
f_{s,12} &= -\frac{\text{sign}(q_s) u_s^{1/2} v_s \gamma_s^{-2} (1 - n \beta_s \cos \theta_B)^{-1}}{1 - u_s \gamma_s^{-2} (1 - n \beta_s \cos \theta_B)^{-2}}, \\
f_{s,\eta} &= -\frac{v_s}{\gamma_s^3 (1 - n \beta_s \cos \theta_B)^2}, \\
\zeta_s &= \frac{n \beta_s \sin \theta_B}{1 - n \beta_s \cos \theta_B},
\end{aligned} \tag{2.13}$$

(the subscript ‘‘0’’ has been suppressed), $n = ck/\omega$ is the refractive index and the relevant dimensionless quantities are

$$u_- = u_+ = u = \frac{\omega_c^2}{\omega^2}, \tag{2.14}$$

$$v_- = \frac{\omega_{p-}^2}{\omega^2}, \quad v_+ = \frac{\omega_{p+}^2}{\omega^2}, \quad v = \frac{\omega_p^2}{\omega^2} = v_- + v_+. \tag{2.15}$$

2.1.1 Pair Plasma With the Same Velocity ($\beta_- = \beta_+ = \beta$)

Consider the case where all the electrons and positrons have the same velocity ($\mathbf{V}_- = \mathbf{V}_+$, $\beta_- = \beta_+ = \beta$, $\gamma_- = \gamma_+ = \gamma$). In this paper, we will focus on the regime where $\omega_c \gg \gamma \omega (1 - n \beta \cos \theta_B)$, or $u \gamma^{-2} (1 - n \beta \cos \theta_B)^{-2} \gg 1$, i.e. the photon frequency shifted to the plasma rest frame is much lower than the cyclotron frequency. In this regime, the components of dielectric tensor can be simplified to

$$\begin{aligned}
S &= 1 + f_{11}, \\
D &= f_{12}, \\
A &= \zeta f_{11}, \\
C &= \zeta f_{12}, \\
P &= 1 + f_\eta + \zeta^2 f_{11},
\end{aligned} \tag{2.16}$$

with

$$\begin{aligned}
f_{11} &= \sum_s f_{s,11} \simeq v u^{-1} \gamma (1 - n \beta \cos \theta_B)^2, \\
f_{12} &= \sum_s f_{s,12} \simeq -(1 - 2f) v u^{-1/2} (1 - n \beta \cos \theta_B), \\
f_\eta &= \sum_s f_{s,\eta} \simeq -v \gamma^{-3} (1 - n \beta \cos \theta_B)^{-2}, \\
\zeta &= n \beta \sin \theta_B (1 - n \beta \cos \theta_B)^{-1}.
\end{aligned} \tag{2.17}$$

2.1.2 Pair Plasma with opposite velocity (the case of $\beta_- = -\beta_+ = \beta$)

Suppose the plasma is composed of two opposite streams: one is the electron stream with $\beta_- = \beta$ and the other is the positron stream with $\beta_+ = -\beta$. For $\omega_c \gg \gamma \omega (1 \pm n \beta \cos \theta_B)$, Eqs. (2.13) simplify to:

$$\begin{aligned}
f_{+,11} &\simeq f v u^{-1} \gamma (1 + n \beta \cos \theta_B)^2, \\
f_{-,11} &\simeq (1 - f) v u^{-1} \gamma (1 - n \beta \cos \theta_B)^2, \\
f_{+,12} &\simeq f v u^{-1/2} (1 + n \beta \cos \theta_B), \\
f_{-,12} &\simeq -(1 - f) v u^{-1/2} (1 - n \beta \cos \theta_B), \\
f_{+,\eta} &\simeq -f v \gamma^{-3} (1 + n \beta \cos \theta_B)^{-2}, \\
f_{-,\eta} &\simeq -(1 - f) v \gamma^{-3} (1 - n \beta \cos \theta_B)^{-2}, \\
\zeta_\pm &= \mp n \beta \sin \theta_B (1 \pm n \beta \cos \theta_B)^{-1}.
\end{aligned} \tag{2.18}$$

2.2 Pair Plasma with a Distribution of γ

The pair plasma in pulsar magnetosphere many have some spread in the Lorentz factors, although the precise distribution is unknown. For a general distribution function $f_s(\gamma_s)$, normalized $\int f_s(\gamma_s) d\gamma_s = 1$, we can average our result in §2.1 to obtain

the dielectric tensor components:

$$\begin{aligned}
S &= 1 + \sum_s \int f_{s,11} f_s(\gamma_s) d\gamma_s, \\
D &= \sum_s \int f_{s,12} f_s(\gamma_s) d\gamma_s, \\
A &= \sum_s \int \zeta_s f_{s,11} f_s(\gamma_s) d\gamma_s, \\
C &= \sum_s \int \zeta_s f_{s,12} f_s(\gamma_s) d\gamma_s, \\
P &= 1 + \sum_s \int (f_{s,\eta} + \zeta_s^2 f_{s,11}) f_s(\gamma_s) d\gamma_s.
\end{aligned} \tag{2.19}$$

These expressions agree with the result derived using standard kinetic theory [e.g. Krall & Trivelpiece 1986, equation (8.10.11); Arons & Barnard 1986; Melrose & Stoneham 1977, Lyutikov 1998].

Given the uncertainty in the γ -distribution, we shall consider the simplest flat distribution, for both electrons and positrons:

$$f(\gamma) = \begin{cases} 1/(2\Delta\gamma) & \gamma_c - \Delta\gamma < \gamma < \gamma_c + \Delta\gamma \\ 0 & \text{otherwise} \end{cases} \tag{2.20}$$

where we shall assume $\gamma_{\min} = \gamma_c - \Delta\gamma \gg 1$ (so that $|\beta| \simeq 1$ for all particles) and $(\gamma_c + \Delta\gamma)\omega(1 \pm n\beta \cos \theta_B) \ll \omega_c$ (so that the Doppler-shifted photon frequency is always below cyclotron resonance). Then the components of the dielectric tensor can be evaluated analytically.

For the case of $\beta_- = \beta_+ = \beta$, substituting Eqs. (2.17) and (2.20) in Eq. (2.19), we obtain

$$\begin{aligned}
S &= 1 + F_{11}, \\
D &= F_{12}, \\
A &= \zeta F_{11}, \\
C &= \zeta F_{12}, \\
P &= 1 + F_\eta + \zeta^2 F_{11},
\end{aligned} \tag{2.21}$$

with

$$F_{11} \simeq v u^{-1} \gamma_c (1 - n\beta \cos \theta_B)^2, \tag{2.22}$$

$$F_{12} \simeq -(1 - 2f) v u^{-1/2} (1 - n\beta \cos \theta_B), \tag{2.23}$$

$$F_\eta = -v \gamma_c^{-3} (1 - \Delta\gamma^2/\gamma_c^2)^{-2} (1 - n\beta \cos \theta_B)^{-2}. \tag{2.24}$$

Note that F_{11} and F_{12} are unchanged compared to the case of delta-function distribution (Eq. 2.17), while F_η is changed by a factor $(1 - \Delta\gamma^2/\gamma_c^2)^{-2}$.

For the case of $\beta_- = -\beta_+ = \beta$, substituting Eqs. (2.13) and (2.20) in Eq. (2.19), we obtain

$$\begin{aligned}
S &= 1 + \sum_s F_{s,11}, \\
D &= \sum_s F_{s,12}, \\
A &= \sum_s \zeta_s F_{s,11}, \\
C &= \sum_s \zeta_s F_{s,12}, \\
P &= 1 + \sum_s (F_{s,\eta} + \zeta_s^2 F_{s,11}),
\end{aligned} \tag{2.25}$$

with

$$F_{+,11} \simeq f v u^{-1} \gamma_c (1 + n\beta \cos \theta_B)^2, \tag{2.26}$$

$$F_{-,11} \simeq (1 - f) v u^{-1} \gamma_c (1 - n\beta \cos \theta_B)^2, \tag{2.27}$$

$$F_{+,12} \simeq f v u^{-1/2} (1 + n\beta \cos \theta_B), \tag{2.28}$$

$$F_{-,12} \simeq -(1-f)vu^{-1/2}(1-n\beta\cos\theta_B), \quad (2.29)$$

$$F_{+,\eta} = -fv\gamma_c^{-3}(1-\Delta\gamma^2/\gamma_c^2)^{-2}(1+n\beta\cos\theta_B)^{-2}. \quad (2.30)$$

$$F_{-,\eta} = -(1-f)v\gamma_c^{-3}(1-\Delta\gamma^2/\gamma_c^2)^{-2}(1-n\beta\cos\theta_B)^{-2}. \quad (2.31)$$

2.3 Correction due to Vacuum Polarization

Vacuum polarization contributes a correction to the dielectric tensor:

$$\Delta\epsilon^{(v)} = (a-1)\mathbf{I} + q\hat{\mathbf{B}}\hat{\mathbf{B}}, \quad (2.32)$$

where \mathbf{I} is the unit tensor and $\hat{\mathbf{B}} = \mathbf{B}/B$ is the unit vector along \mathbf{B} (here we use $\mathbf{B}, \hat{\mathbf{B}}$ to denote $\mathbf{B}_0, \hat{\mathbf{B}}_0$ for simple notations). The magnetic permeability tensor $\boldsymbol{\mu}$ also deviates from unity because of vacuum polarization, with the inverse permeability given by

$$\boldsymbol{\mu}^{-1} = a\mathbf{I} + m\hat{\mathbf{B}}\hat{\mathbf{B}}. \quad (2.33)$$

In the low frequency limit $\hbar\omega \ll m_e c^2$, general expressions for the vacuum polarization coefficients a, q , and m are given in Adler (1971) and Heyl & Hernquist (1997). For $B \ll B_Q = m_e^2 c^3 / (e\hbar) = 4.414 \times 10^{13}$ G, they are given by

$$a = 1 - 2\delta_V, \quad q = 7\delta_V, \quad m = -4\delta_V, \quad (2.34)$$

where

$$\delta_V = \frac{\alpha_F}{45\pi} \left(\frac{B}{B_Q} \right)^2 = 2.650 \times 10^{-8} B_{12}^2 \quad (2.35)$$

and $\alpha_F = e^2/\hbar c = 1/137$ is the fine structure constant. For $B \gg B_Q$, simple expressions for a, q, m are given in Ho & Lai (2003) (see also Potekhin et al. 2004 for general fitting formulae).

When $|\Delta\epsilon_{ij}^{(v)}| \ll 1$ or $B/B_Q \ll 3\pi/\alpha_F$ ($B \ll 5 \times 10^{16}$ G), the plasma and vacuum contributions to the dielectric tensor can be added linearly, i.e., $\epsilon = \epsilon^{(p)} + \Delta\epsilon^{(v)}$. In the frame with $\hat{\mathbf{B}}$ along $\hat{\mathbf{z}}'$,

$$[\epsilon]_{\hat{\mathbf{z}}'=\hat{\mathbf{B}}} = \begin{bmatrix} S' & iD & A \\ -iD & S' & -iC \\ A & iC & P' \end{bmatrix}, \quad (2.36)$$

with $S' = S + \hat{a}$, $P' = P + \hat{a} + q$ and $\hat{a} = a - 1$,

3 WAVE MODES IN A COLD STREAMING PLASMA

Here we consider the case of a pair plasma all streaming with the same velocity β along the field line. The effect of finite spread in γ will be studied in §5, and the case of opposite streams will be considered in §6.

3.1 Equations for the Wave Modes

Using the electric displacement $\mathbf{D} = \epsilon \cdot \mathbf{E}$ and equation (2.33) in the Maxwell equations, we obtain the equation for plane waves with $\mathbf{E} \propto e^{i(\mathbf{k}\cdot\mathbf{r}-\omega t)}$ (henceforth we use \mathbf{E} to denote $\delta\mathbf{E}$, and use \mathbf{B} to denote \mathbf{B}_0)

$$\left\{ \frac{1}{a}\epsilon_{ij} + n^2 \left[\hat{k}_i \hat{k}_j - \delta_{ij} - \frac{m}{a} (\hat{k} \times \hat{B})_i (\hat{k} \times \hat{B})_j \right] \right\} E_j = 0, \quad (3.37)$$

where $n = ck/\omega$ is the refractive index and $\hat{\mathbf{k}} = \mathbf{k}/k$. In the coordinate system xyz with \mathbf{k} along the z -axis and \mathbf{B} in the xz -plane, such that $\hat{\mathbf{k}} \times \hat{\mathbf{B}} = -\sin\theta_B \hat{\mathbf{y}}$, the components of dielectric tensor are given by [compared to eq. (2.36)]

$$\begin{aligned} \epsilon_{xx} &= S' \cos^2 \theta_B - 2A \sin \theta_B \cos \theta_B + P' \sin^2 \theta_B, \\ \epsilon_{yy} &= S', \\ \epsilon_{zz} &= S' \sin^2 \theta_B + 2A \sin \theta_B \cos \theta_B + P' \cos^2 \theta_B, \\ \epsilon_{xy} &= -\epsilon_{yx} = i(D \cos \theta_B - C \sin \theta_B), \\ \epsilon_{zx} &= \epsilon_{xz} = A \cos 2\theta_B + (S' - P') \sin \theta_B \cos \theta_B, \\ \epsilon_{yz} &= -\epsilon_{zy} = -i(D \sin \theta_B + C \cos \theta_B), \end{aligned} \quad (3.38)$$

The z -component of equation (3.37) gives

$$E_z = -\epsilon_{zz}^{-1} (\epsilon_{zx} E_x + \epsilon_{zy} E_y). \quad (3.39)$$

Reinserting this back into equation (3.37) yields

$$\begin{pmatrix} \eta_{xx} - n^2 & \eta_{xy} \\ \eta_{yx} & \eta_{yy} - rn^2 \end{pmatrix} \begin{pmatrix} E_x \\ E_y \end{pmatrix} = 0, \quad (3.40)$$

where $r = 1 + \hat{r} \equiv 1 + (m/a) \sin^2 \theta_B$ and

$$\eta_{xx} = \frac{1}{a\epsilon_{zz}} (\epsilon_{zz}\epsilon_{xx} - \epsilon_{xz}\epsilon_{zx}) = \frac{1}{a\epsilon_{zz}} (S'P' - A^2), \quad (3.41)$$

$$\begin{aligned} \eta_{yy} &= \frac{1}{a\epsilon_{zz}} (\epsilon_{zz}\epsilon_{yy} - \epsilon_{yz}\epsilon_{zy}) \\ &= \frac{1}{a\epsilon_{zz}} [(S'^2 - D^2 - S'P' + C^2) \sin^2 \theta_B + 2(AS' - CD) \sin \theta_B \cos \theta_B + S'P' - C^2], \end{aligned} \quad (3.42)$$

$$\begin{aligned} \eta_{yx} &= -\eta_{xy} = \frac{1}{a\epsilon_{zz}} (\epsilon_{zz}\epsilon_{yx} - \epsilon_{yz}\epsilon_{zx}) \\ &= \frac{-i}{a\epsilon_{zz}} [P'D \cos \theta_B - S'C \sin \theta_B + A(D \sin \theta_B - C \cos \theta_B)]. \end{aligned} \quad (3.43)$$

3.2 $B = \infty$ limit without QED effect

The above expressions are valid for the general dielectric tensor (Eq. 2.36). We now consider the $B = \infty$ limit introduced by e.g., Tsytovitch & Kaplan (1972) and Arons & Barnard (1986). In this regime, the magnetic field is sufficiently large so that the cyclotron frequency are large compared to the Lorentz-shifted wave frequency. At the same time, B is not really infinity so that the wave propagation is dominated by plasma effect and we neglect the QED correction in the dielectric tensor. The approximate elements of the dielectric tensor are

$$f_{11} \sim vu^{-1}\gamma \sim 0, \quad f_{12} \sim -(1 - 2f)vu^{-1/2} \sim 0, \quad (3.44)$$

$$f_\eta \simeq -v\gamma^{-3} (1 - n\beta \cos \theta_B)^{-2}, \quad (3.45)$$

$$S \simeq 1, \quad P \simeq 1 + f_\eta, \quad D \simeq 0, \quad A \simeq 0, \quad C \simeq 0, \quad (3.46)$$

$$\epsilon_{zz} \simeq 1 + f_\eta \cos^2 \theta_B. \quad (3.47)$$

Equations (3.41) – (3.43) then reduce to

$$\begin{aligned} \eta_{xx} &\simeq \frac{1 + f_\eta}{1 + f_\eta \cos^2 \theta_B}, \\ \eta_{yy} &\simeq 1, \\ \eta_{yx} &\simeq -\eta_{xy} \simeq 0. \end{aligned} \quad (3.48)$$

Solving equation (3.40), we find (see Arons & Barnard 1986)

$$n^2 = \eta_{xx} = \frac{1 + f_\eta}{1 + f_\eta \cos^2 \theta_B} \quad (3.49)$$

or

$$(\omega^2 - c^2 k_\parallel^2) \left[1 - \frac{\omega_p^2}{\gamma^3 \omega^2 (1 - \beta c k_\parallel / \omega)^2} \right] - c^2 k_\perp^2 = 0 \quad (3.50)$$

(where $k_\parallel = k \cos \theta_B$, $k_\perp = k \sin \theta_B$) for the ordinary mode (O-mode) and

$$n^2 = 1 \quad (3.51)$$

for the extraordinary mode (X-mode). The polarization of the O-mode is given by

$$\left| \frac{E_y}{E_x} \right| = \left| \frac{\eta_{yx}}{\eta_{yy} - \eta_{xx}} \right| \sim 0, \quad (3.52)$$

$$\left| \frac{E_z}{E_x} \right| = \left| \frac{f_\eta \sin \theta_B \cos \theta_B}{1 + f_\eta \cos^2 \theta_B} \right| = \left| \frac{n^2 - 1}{\tan \theta_B} \right|, \quad (3.53)$$

and that for the X mode is

$$\left| \frac{E_x}{E_y} \right| \sim 0, \quad \left| \frac{E_z}{E_y} \right| \sim 0. \quad (3.54)$$

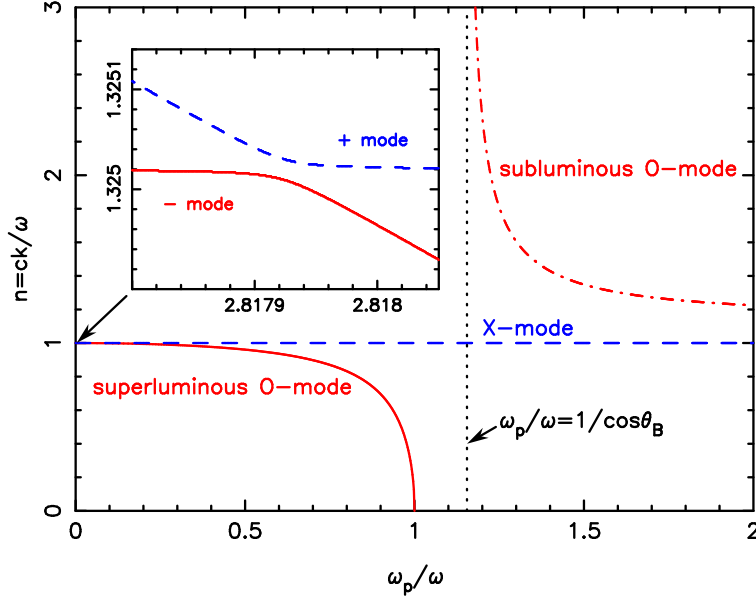


Figure 1. The refractive indices $n = ck/\omega$ of wave modes as a function of ω_p/ω for a cold plasma with $\gamma = 1$ and the wave propagation angle $\theta_B = 30^\circ$. The solid line shows the superluminous O-mode, the dashed line the X-mode, and the dot-dashed line the subluminal O-mode. The insert shows the blowup of the “avoided crossing” region between the X-mode and the superluminous O-mode due to vacuum resonance. The mixed modes are labeled “+” mode and “-” mode. For the insert, the x -axis gives $10^4 \omega_p/\omega$, and y -axis gives $10^8(n - 1)$, and the other parameters are $B = 10^{12}$ G, $N = N_{GJ}$ with $P = 1$ s.

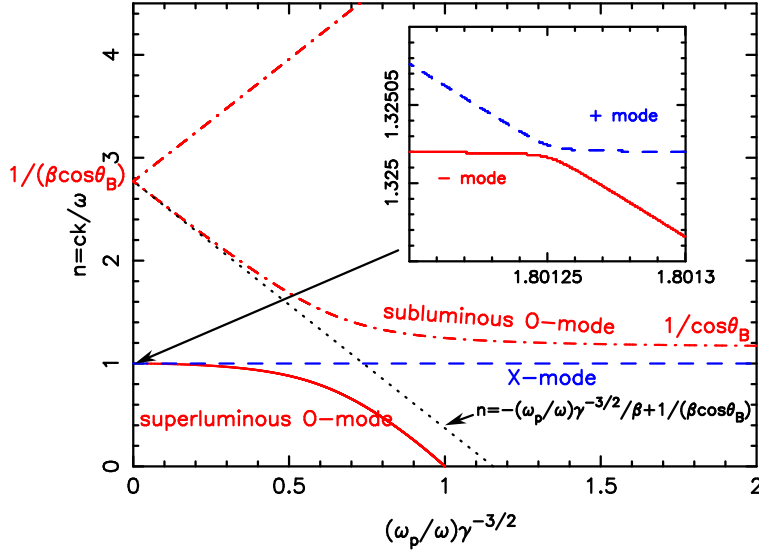


Figure 2. Same as Fig.1 except for $\gamma = 1.1$, and the x -axis gives $(\omega_p/\omega)\gamma^{-3/2}$. Note that for $(\omega_p/\omega)\gamma^{-3/2} \ll 1$, the subluminal O-mode has $n = -(\omega_p/\omega)\gamma^{-3/2}/\beta + 1/(\beta \cos \theta_B)$, and it is shown as a dotted line in the figure.

Thus, the X-mode is a transverse wave with the electric field vector in the $\mathbf{k} \times \mathbf{B}$ direction, while the O-mode is polarized in the plane spanned by \mathbf{k} and \mathbf{B} .

Figures 1 – 3 depict the refractive indices $n = ck/\omega$ of different modes as a function of $(\omega_p/\omega)\gamma^{-3/2}$ for $\gamma = 1, 1.1$ and 10^3 , respectively, all with $\theta_B = 30^\circ$. The O-modes have two branches: the superluminous branch ($w > ck$ or $n < 1$) and the subluminal branch ($w < ck$ or $n > 1$), the latter corresponds to plasma oscillations. At low densities, $(\omega_p/\omega)\gamma^{-3/2} \ll 1$, the superluminous O-mode becomes transverse vacuum electromagnetic wave which can escape from the magnetosphere.

In the very low density region, $(\omega_p/\omega)\gamma^{-3/2} \ll 1$, the QED effect may not be neglected compared to the plasma effect. The “competition” between the vacuum polarization effect and the plasma effect gives rise to a vacuum resonance, at which the superluminous O-mode and the X-mode may be coupled with each other. In the remainder of this paper, we will focus on this vacuum resonance phenomenon.

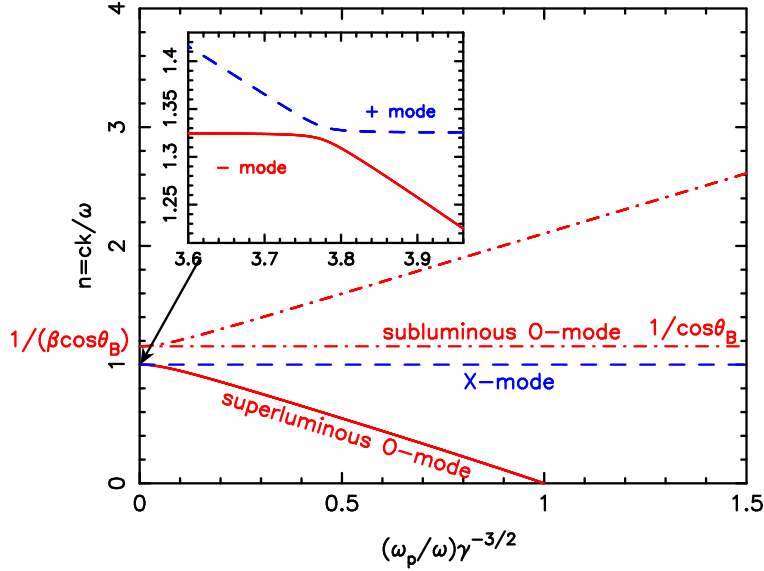


Figure 3. Same as Figure 2 except for $\gamma = 10^3$. In the insert, the x-axis gives $10^5(\omega_p/\omega)\gamma^{-3/2}$ and the y-axis $10^8(n-1)$.

3.3 Wave Modes Including QED Effect

We now consider how vacuum polarization affects the X-mode and (superluminous) O-mode. Because of the possibility of “mode crossing”, we label the modes as “+ mode” and “- mode”. We write the mode polarization vector as $\mathbf{E}_\pm = \mathbf{E}_{\pm T} + \mathbf{E}_{\pm z}\hat{z}$, with the transverse part

$$\mathbf{E}_{\pm T} = \frac{1}{(1 + K_\pm^2)^{1/2}}(iK_\pm, 1), \quad (3.55)$$

where $iK_\pm = E_x/E_y$. Eliminating n^2 from equation (3.40), we obtain

$$K_\pm = \beta_p \pm \sqrt{\beta_p^2 + r} \simeq \beta_p \pm \sqrt{\beta_p^2 + 1}, \quad (3.56)$$

where the polarization parameter β_p is given by

$$\begin{aligned} \beta_p &= -i \frac{r\eta_{xx} - \eta_{yy}}{2\eta_{yx}} \\ &= -\frac{(S'^2 - D^2 - S'P' + C^2)\sin^2\theta_B + (A^2 - C^2) + (AS' - DC)\sin 2\theta_B + (S'P' - A^2)(1-r)}{2[P'D\cos\theta_B - S'C\sin\theta_B + A(D\sin\theta_B - C\cos\theta_B)]}. \end{aligned} \quad (3.57)$$

The index of refraction n_\pm of the two modes can be obtained from equation (3.40), giving

$$n_\pm^2 = \frac{\eta_{yy}}{r} + \frac{\eta_{yx}}{r}iK_\pm. \quad (3.58)$$

We now consider the case of cold streaming plasma with $\beta_- = \beta_+ = \beta$. We focus on parameter regimes satisfying the following conditions:

$$u\gamma^{-2}(1 - \beta\cos\theta_B)^{-2} = 7.812 \times 10^{12} B_{12}^2 \nu_1^{-2} \gamma_3^{-2} (1 - \beta\cos\theta_B)^{-2} \gg 1, \quad (3.59)$$

$$v\gamma^{-1} = 5.617 \times 10^{-3} \eta B_{12} P_1^{-1} \nu_1^{-2} \gamma_3^{-1} \ll 1, \quad (3.60)$$

where ν is the wave (photon) frequency, $\nu_1 = \nu/(1\text{ GHz})$ and $\gamma_3 = \gamma/10^3$. The first condition implies that the Doppler-shifted frequency is lower than ω_c , so that we can use equation (2.17) for f_{11} , f_{12} and f_η . The second condition implies $|f_{12}|^2 \ll |f_{11}| \ll 1$, and $|f_\eta| \ll 1$. Under these conditions, equation (3.57) reduces to

$$\beta_p \simeq \frac{(f_\eta + q + m)\sin^2\theta_B - f_{11}[1 - (\cos\theta_B - \zeta\sin\theta_B)^2]}{2f_{12}(\cos\theta_B - \zeta\sin\theta_B)}. \quad (3.61)$$

We shall see that conditions (3.59) and (3.60) also imply that the index of refraction is close to unity, $|n-1| \ll 1$. Thus $(\cos\theta_B - \zeta\sin\theta_B)^2 = (\cos\theta_B - n\beta)^2/(1 - n\beta\cos\theta_B)^2 \approx 1 - \gamma^{-2}\sin^2\theta_B(1 - \beta\cos\theta_B)^2$, and we can easily check that the second term in the numerator of equation (3.61) is much smaller than f_η . Equation (3.61) therefore simplifies to

$$\beta_p \simeq \frac{f_\eta + q + m}{2f_{12}} \frac{\sin^2\theta_B}{(\cos\theta_B - \zeta\sin\theta_B)}$$

$$\begin{aligned}
&= \frac{f_\eta}{2f_{12}} \frac{\sin^2 \theta_B}{(\cos \theta_B - \zeta \sin \theta_B)} \left(1 + \frac{q+m}{f_\eta} \right) \\
&= \beta_0 \beta_V,
\end{aligned} \tag{3.62}$$

where β_0 is the polarization parameter in the absence of vacuum polarization:

$$\begin{aligned}
\beta_0 &\simeq \frac{f_\eta}{2f_{12}} \frac{\sin^2 \theta_B}{(\cos \theta_B - \zeta \sin \theta_B)} \\
&\simeq -\frac{1}{2} (1-2f)^{-1} u^{1/2} \gamma^{-3} (1-\beta \cos \theta_B)^{-3} \frac{\sin^2 \theta_B}{(\cos \theta_B - \zeta \sin \theta_B)},
\end{aligned} \tag{3.63}$$

and β_V is the correction factor due to vacuum polarization:

$$\begin{aligned}
\beta_V &\simeq 1 + \frac{q+m}{f_\eta} \\
&\simeq 1 - \frac{q+m}{v\gamma^{-3} (1-\beta \cos \theta_B)^{-2}}.
\end{aligned} \tag{3.64}$$

Equation (3.58) for the index of refraction n_\pm of the two modes also simplifies to

$$n_\pm^2 \simeq 1 - m \sin^2 \theta_B + f_{11} + f_{12} (\cos \theta_B - \zeta \sin \theta_B) K_\pm. \tag{3.65}$$

For positive β_p with $|\beta_p| \gg 1$, we obtain simple expressions of refractive indices

$$n_+^2 = 1 - m \sin^2 \theta_B + f_{11} + (f_\eta + q + m) \sin^2 \theta_B, \quad n_-^2 = 1 - m \sin^2 \theta_B + f_{11}, \tag{3.66}$$

while for negative β_p with $|\beta_p| \gg 1$, we have

$$n_+^2 = 1 - m \sin^2 \theta_B + f_{11}, \quad n_-^2 = 1 - m \sin^2 \theta_B + f_{11} + (f_\eta + q + m) \sin^2 \theta_B. \tag{3.67}$$

For $|\beta_p| = 0$, we have $K_\pm = \pm 1$ and

$$n_\pm^2 = 1 - m \sin^2 \theta_B + f_{11} \pm f_{12} (\cos \theta_B - \zeta \sin \theta_B). \tag{3.68}$$

From equations (3.66–3.68), we see that n is indeed close to unity when equations (3.59) and (3.60) are satisfied.

3.4 Vacuum Resonance

For $|\beta_p| \gg 1$, the two modes are (almost) linearly polarized: the mode with $|K| \simeq 2|\beta_p| \gg 1$ is polarized in the $\hat{\mathbf{k}}\text{-}\hat{\mathbf{B}}$ plane, and is usually called ordinary mode (O-mode); the mode with $|K| \simeq 1/(2|\beta_p|) \ll 1$ is polarized perpendicular to the $\hat{\mathbf{k}}\text{-}\hat{\mathbf{B}}$ plane, and is called extraordinary mode (X-mode). From equation (3.62), we see that for a general θ_B which is not too close to 0° or 180° , and for almost all values of B , N , ν , γ 's, the inequality $|\beta_p| \gg 1$ is satisfied either when the condition

$$\begin{aligned}
\left| \frac{f_\eta}{f_{12}} \sin^2 \theta_B \right| &\simeq (1-2f)^{-1} u^{1/2} \gamma^{-3} (1-\cos \theta_B)^{-3} \sin^2 \theta_B \\
&= 2.795 B_{12} \nu_1^{-1} \gamma_3^{-3} (1-\cos \theta_B)^{-3} \sin^2 \theta_B (1-2f)^{-1} \gg 1
\end{aligned} \tag{3.69}$$

is satisfied, or when

$$\begin{aligned}
\left| \frac{q+m}{f_{12}} \sin^2 \theta_B \right| &\simeq \frac{\alpha_F}{15\pi} \left(\frac{B}{B_Q} \right)^2 (1-2f)^{-1} u^{1/2} v^{-1} (1-\cos \theta_B)^{-1} \sin^2 \theta_B \\
&= 39.56 B_{12}^2 \nu_1 (1-2f)^{-1} \eta^{-1} P_1 (1-\cos \theta_B)^{-1} \sin^2 \theta_B \gg 1
\end{aligned} \tag{3.70}$$

is satisfied. The exception occurs when

$$f_\eta + q + m = 0 \tag{3.71}$$

or

$$\beta_V = 1 - \frac{q+m}{v\gamma^{-3} (1-\beta \cos \theta_B)^{-2}} = 0. \tag{3.72}$$

This defines the ‘‘vacuum resonance’’. For given ν , γ and B , the resonance occurs at the density

$$N_V = 9.905 \times 10^{11} B_{12}^2 \nu_1^2 \gamma_3^3 (1-\beta \cos \theta_B)^2 F(b) \text{ cm}^{-3}, \tag{3.73}$$

where

$$F(b) \equiv \frac{q+m}{\alpha_F^2 b^2 / (15\pi)} \tag{3.74}$$

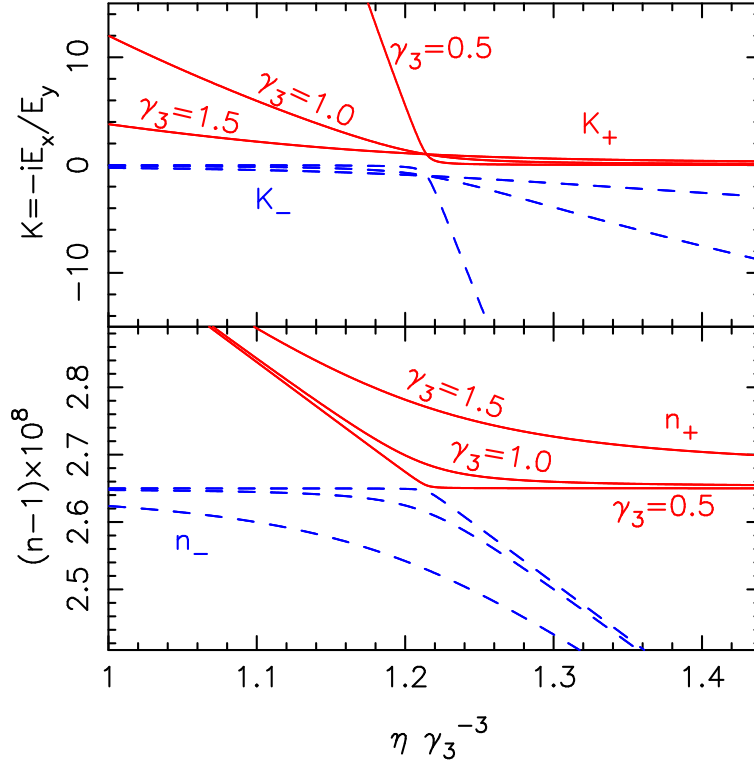


Figure 4. The polarization ellipticity K (upper panel) and index of refraction n (lower panel) of the wave mode as a function of the plasma density parameter $\eta = N/N_{\text{GJ}}$ (see equation 2.2) near the vacuum resonance for $B = 10^{12}$ G, $\nu = 1$ GHz, $f = 0$ and $\theta_B = 45^\circ$. Three values of γ are considered: $\gamma_3 = \gamma/10^3 = 0.5, 1, 1.5$. The solid lines are for the “+” mode and dashed lines for the “-” mode. Both the resonant density (see Eq. 3.75) and width (see Eq. 3.77) are proportional to γ^3 for $\gamma \gg 1$.

is equal to unity for $b = B/B_Q \ll 1$ and is at most of order a few for $B \lesssim 10^{15}$ G (see Fig. 1 of Ho & Lai 2003). It’s obvious that $N_V \propto \gamma^3$ for $\gamma \gg 1$ and θ_B not too close to 0° (see Figure 4). For $\gamma = 1$, equation (3.73) agrees with the result of Lai & Ho (2002). The dependence of the resonance density N_V on γ and θ_B can be easily understood from the cold (non-streaming) plasma limit and Lorentz transform. The wave frequency in the plasma rest frame is $\omega' = \gamma(\omega - \beta k_{\parallel}) \simeq \gamma\omega(1 - \beta \cos \theta_B)$. Note that in this frame, the external magnetic field and the dielectric tensor due to vacuum polarization are unchanged. The rest frame plasma density at the vacuum resonance is $N'_V \propto B^2 \omega'^2 F(b)$, and the corresponding “lab frame” density is $N_V = \gamma N'_V$. We can rewrite the resonance density in terms of the Goldreich-Julian density

$$\eta_V = \frac{N_V}{N_{\text{GJ}}} = 14.15 P_1 B_{12}^{-1} \nu_1^2 \gamma_3^3 (1 - \beta \cos \theta_B)^2 F(b). \quad (3.75)$$

The physical meaning of the resonance is clear: For given ν , γ and B , the dielectric property of the medium is dominated by the plasma effect when $N \gg N_V$, while it is dominated by vacuum polarization when $N \ll N_V$; at $N = N_V$, the plasma effect and vacuum polarization compensate each other, and the wave modes become exactly circular polarized.

There are other ways to view the vacuum resonance. For example, at given B , γ and density N (or η), we can define the vacuum resonance frequency:

$$\nu_V = 0.266 [P_1^{-1} B_{12}^{-1} \eta \gamma_3^{-3} (1 - \beta \cos \theta_B)^{-2} F^{-1}]^{1/2} \text{ GHz}. \quad (3.76)$$

Thus, wave modes with $\nu \ll \nu_V$ are determined by the plasma effect, while those with $\nu \gg \nu_V$ are determined by the vacuum polarization effect.

The characteristic width of the resonance region can be estimated by considering $|\beta_p| = 1$ as defining the edge of the resonance. Since $\beta_V = 1 - N_V/N$, we find that the densities at the edges of the resonance are $N_V \pm \Delta N$, with

$$\frac{\Delta N}{N_V} \simeq \frac{1}{|\beta_0|} = 0.7157 (1 - 2f) B_{12}^{-1} \nu_1 \gamma_3^3 (1 - \beta \cos \theta_B)^3 \frac{(\cos \theta_B - \zeta \sin \theta_B)}{\sin^2 \theta_B}, \quad (3.77)$$

where $\cos \theta_B - \zeta \sin \theta_B \simeq (\cos \theta_B - \beta)/(1 - \beta \cos \theta)$.

Figures 4 and 5 show the mode properties near vacuum resonance for different values of γ and f . It’s obvious that the resonance density and width scale with γ^3 (for $\gamma \gg 1$), and the resonance density doesn’t change with f , while the resonance region becomes narrow when f is close to 0.5.

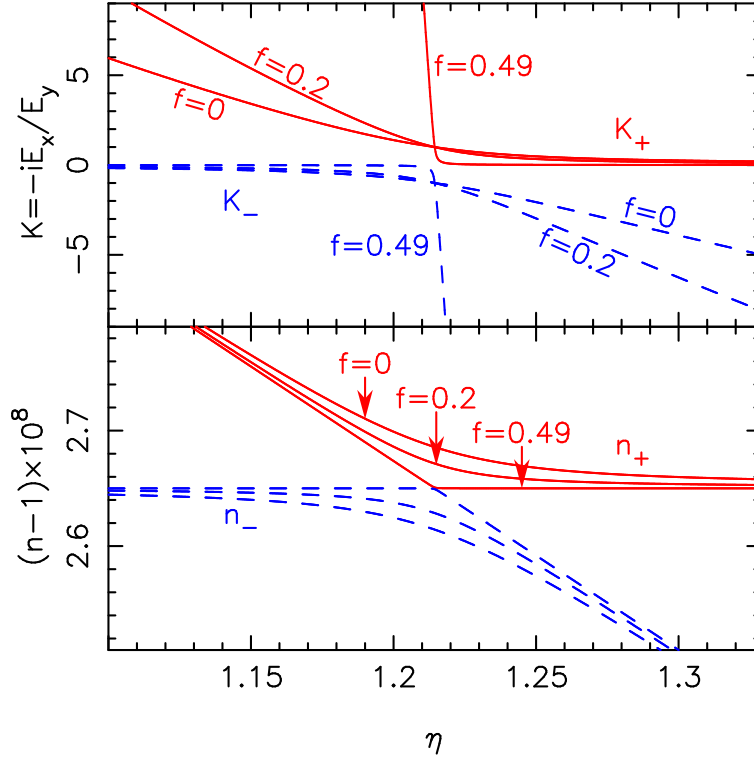


Figure 5. Same as Fig. 4, except for $B = 10^{12}$ G, $\nu = 1$ GHz, $\gamma = 10^3$, $\theta_B = 45^\circ$ and different values of the plasma positron fraction: $f = 0, 0.2$ and 0.49 .

Note that while vacuum resonance can always be located by $f_\eta + q + m = 0$ [Eqs. (3.71) and (3.72)], significant “avoided mode crossing” (as illustrated in Figs. 4 and 5 and the inserts of Figs. 1 – 3) occurs only if equations (3.69) and (3.70) are satisfied. If these “linear polarization” conditions are not satisfied, the modes will be approximately circular polarized even away from the resonance, and no dramatic change in the mode properties takes place around the vacuum resonance (see Fig. 6).

4 MODE EVOLUTION ACROSS THE VACUUM RESONANCE

Consider a photon (or electromagnetic wave) of a given frequency ν and polarization state propagating in the NS magnetosphere. The magnetosphere is inhomogeneous because of variations in \mathbf{B} , N and possibly γ . How does the polarization of the photon evolve, particularly as the photon traverses the vacuum resonance region (e.g. from the plasma-dominated region to the vacuum-dominated region)? Clearly, if the variations of the magnetosphere parameters (\mathbf{B} , N , etc.) are sufficiently gentle, the polarization state of the photon will evolve adiabatically, i.e. a photon in a definite wave mode will stay in that mode. Then Figure 4 and 5 show that across the vacuum resonance, the photon polarization ellipse will rotate by 90° , with the mode helicity unchanged.

To quantify the mode evolution, it is convenient to introduce the “mixing” angle θ_m via $\tan \theta_m = 1/K_+$, so that

$$\tan 2\theta_m = \beta_p^{-1}, \quad (4.78)$$

where we have used $|r - 1| \ll 1$. The transverse eigenvectors of the modes are $\mathbf{E}_{+T} = (i \cos \theta_m, \sin \theta_m)$ and $\mathbf{E}_{-T} = (-i \sin \theta_m, \cos \theta_m)$. Clearly, at the resonance, $\theta_m = 45^\circ$, the X-mode and O-mode are maximally “mixed”.

A general polarized electromagnetic wave with frequency ω traveling in the z -direction can be written as a superposition of the two modes:

$$\mathbf{E}(z) = A_+(z)\mathbf{E}_+(z) + A_-(z)\mathbf{E}_-(z), \quad (4.79)$$

Note that both A_\pm and \mathbf{E}_\pm depend on z . Substituting equation (4.79) into the wave equation

$$\nabla \times (\boldsymbol{\mu}^{-1} \cdot \nabla \times \mathbf{E}) = \frac{\omega^2}{c^2} \boldsymbol{\epsilon} \cdot \mathbf{E}, \quad (4.80)$$

we obtain the amplitude evolution equations (see Lai & Ho 2002)

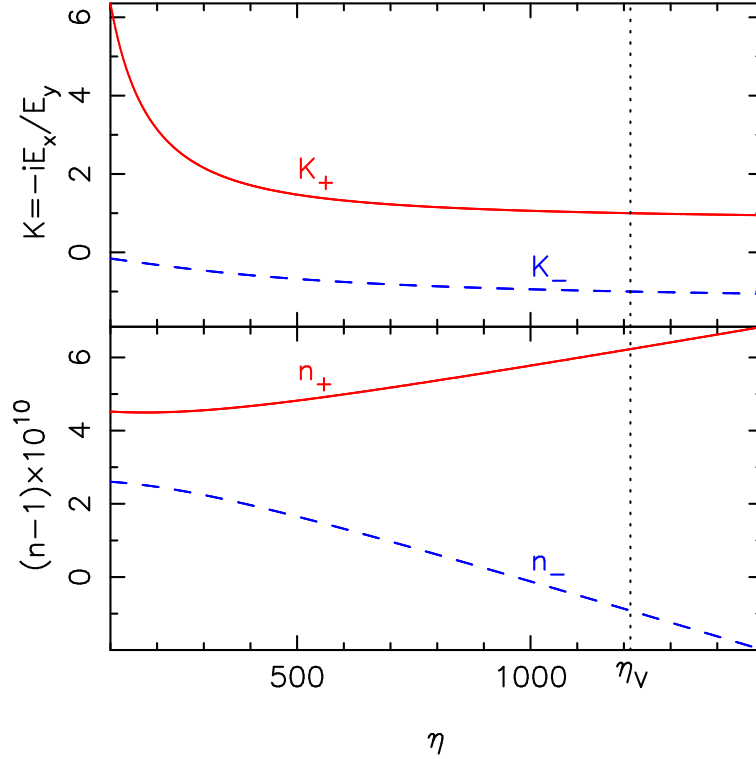


Figure 6. Same as Fig. 4, except for $B = 10^{11}$ G, $\nu = 100$ GHz, $1 - 2f = 0.1$, $\gamma = 10^3$, $\theta_B = 45^\circ$. The vacuum resonance (defined by $f_\eta + q + m = 0$) occurs at $\eta = 1.214 \times 10^3$ (the vertical dotted line). In this case, equations (3.69) and (3.70) are not satisfied, and “avoided mode crossing” does not occur near the vacuum resonance.

$$i \begin{pmatrix} A'_+ \\ A'_- \end{pmatrix} \simeq \begin{pmatrix} -\Delta k/2 & i\theta'_m \\ -i\theta'_m & \Delta k/2 \end{pmatrix} \begin{pmatrix} A_+ \\ A_- \end{pmatrix}, \quad (4.81)$$

where $'$ stands for d/dz , $\Delta k = k_+ - k_-$. In deriving equation (4.81), we have assumed that $\mathbf{E}_\pm(z)$ and $A_\pm(z)\exp(-i \int^z k_\pm dz)$ vary on a length scale much larger than the photon wavelength, and we have used $k_+ \simeq k_-$ and $|k'_\pm/k_\pm| \ll |k_\pm|$. Clearly, when $|\theta'_m| \ll |\Delta k/2|$, or

$$\Gamma \equiv \left| \frac{(n_+ - n_-)\omega}{2\theta'_m c} \right| \gg 1, \quad (4.82)$$

the polarization vector will evolve adiabatically (e.g., a photon in the plus-mode will remain in the plus-mode). Using equations (3.62) and (4.78), we find

$$\theta'_m = -\frac{1}{4} \sin^2 2\theta_m \frac{f_\eta}{f_{12}} \frac{\sin^2 \theta_B}{(\cos \theta_B - \zeta \sin \theta_B)} \frac{\beta'_p}{\beta_0}. \quad (4.83)$$

The difference in refractive indices of the two modes is

$$n_+ - n_- \simeq \frac{f_{12} (\cos \theta_B - \zeta \sin \theta_B)}{\sin 2\theta_m}. \quad (4.84)$$

Thus equation (4.82) becomes

$$\Gamma = \frac{2\omega H}{c} (1 - 2f)^2 \frac{\gamma^3 \omega_p^2}{\omega_c^2 \sin^3(2\theta_m)} (1 - \beta \cos \theta_B)^4 \left(\frac{\cos \theta_B - \zeta \sin \theta_B}{\sin \theta_B} \right)^2 \gg 1, \quad (4.85)$$

where $H \equiv |\beta_0/\beta'_p|$ specifies the length scale of variation of β_p along the ray. Equation (4.85) gives the general condition for adiabatic mode evolution along the photon path.

Clearly, the adiabatic condition (4.82) or (4.85) is most easily violated at the resonance ($\theta_m = 45^\circ$). Evaluating equation (4.85) at $N = N_V$ and using equation (3.72) to eliminate ω_p^2 , we obtain

$$\Gamma_V = (\nu/\nu_{\text{ad}})^3, \quad (4.86)$$

with the “adiabatic frequency”

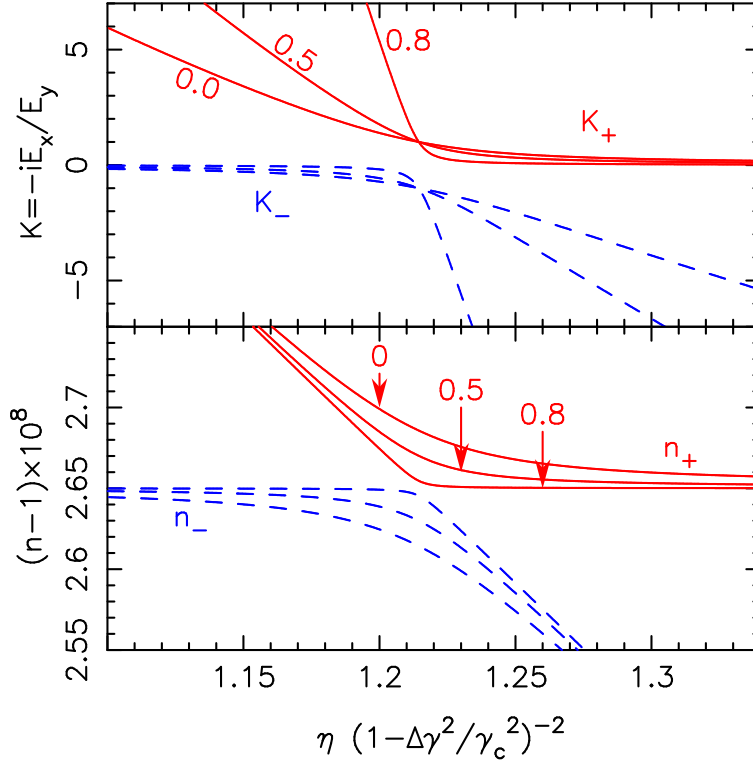


Figure 7. Same as Fig. 4, except for plasmas with a flat distribution of Lorentz factor (see equation 2.20). The parameters are $B = 10^{12}$ G, $\nu = 1$ GHz, $f = 0$, $\gamma = 10^3$, $\theta_B = 45^\circ$. For each mode, the three lines are for $\Delta\gamma/\gamma_c = 0, 0.5, 0.8$.

$$\nu_{\text{ad}} = 6.081 (1 - 2f)^{-2/3} \gamma_3^{-2} (1 - \beta \cos \theta_B)^{-2} F^{-1/3} \left(\frac{\sin \theta_B}{\cos \theta_B - \zeta \sin \theta_B} \right)^{2/3} H_6^{-1/3} \text{ GHz}, \quad (4.87)$$

where we have used $H \simeq |dz/d\beta_V|$ and $H_6 = H/(10^6 \text{ cm})$. Since $\beta_V = (1 - N_V/N)$ and β_0 changes very slowly near resonance, for a constant \mathbf{B} , γ , the length $H = N/|dN/dz|$ (evaluated at $N = N_V$) becomes the density scale height along the ray. For $\gamma = 1$, equations (4.86) and (4.87) agree with the result of Lai & Ho (2002). Using equation (3.76) to eliminate γ , we can also rewrite equation (4.87) as

$$\nu_{\text{ad}} \simeq 35.59 (1 - 2f)^{-2/3} \nu_1^{4/3} \eta^{-2/3} (P_1 B_{12})^{2/3} F^{1/3} H_6^{-1/3} (1 - \beta \cos \theta_B)^{-2/3} \left(\frac{\sin \theta_B}{\cos \theta_B - \zeta \sin \theta_B} \right)^{2/3} \text{ GHz}. \quad (4.88)$$

5 THE INFLUENCE OF VELOCITY DISTRIBUTION

The results of Sections 3 and 4 are for cold streaming plasma with a single Lorentz factor γ . For a general distribution function $f(\gamma)$, equations (3.37) – (3.43) and equations (3.55) – (3.58) still apply. For the simplest flat distribution of γ [Eq. (2.20)], the dielectric tensor functions are given by equation (2.22) – (2.24) for $\gamma_{\text{min}} \gg 1$ and $\gamma_{\text{max}} \omega (1 - n\beta \cos \theta_B) \ll \omega_c$. If we assume $v\gamma_{\text{min}}^{-1} \ll 1$ [see Eq. (3.60)], so that $n_{\pm} \simeq 1$, we find that the vacuum resonance density, width and adiabatic frequency are given by:

$$\eta_V = \frac{N_V}{n_{GJ}} = 14.15 P_1 B_{12} \nu_1^2 \gamma_c^3 (1 - \Delta\gamma^2/\gamma_c^2)^2 (1 - \beta \cos \theta_B)^2 F, \quad (5.89)$$

$$\frac{\Delta N}{N_V} = 0.7157 (1 - 2f) B_{12}^{-1} \gamma_c^3 (1 - \Delta\gamma^2/\gamma_c^2)^2 (1 - \beta \cos \theta_B)^3 \frac{(\cos \theta_B - \zeta \sin \theta_B)}{\sin^2 \theta_B}, \quad (5.90)$$

$$\nu_{\text{ad}} = 6.081 (1 - 2f)^{-2/3} \gamma_3^{-2} (1 - \beta \cos \theta_B)^{-2} F^{-1/3} \left(\frac{\sin \theta_B}{\cos \theta_B - \zeta \sin \theta_B} \right)^{2/3} H_6^{-1/3} \text{ GHz}. \quad (5.91)$$

Figure 7 shows the polarization ellipticities and the refractive indices of the two wave modes in plasmas with different $\Delta\gamma$'s. Thus, a broad distribution of γ 's does not qualitatively affect the vacuum resonance behavior.

6 VACUUM RESONANCE IN A PLASMA WITH TWO OPPOSITE STREAMS

We now consider the case where the pair plasma is composed of two opposite streams, for which the dielectric tensor is given in Sec.2.1.2. The derivation of mode properties for this case are the same as in Section 3. Similar to Eqs. (3.59) and (3.60), we assume $u\gamma^{-2}(1 \pm n\beta \cos \theta_B)^{-2} \gg 1$ and $v\gamma^{-1} \ll 1$. The polarization parameter β_p (Eq. 3.57) reduces to

$$\beta_p \simeq \frac{(f_{\eta,+} + f_{\eta,-} + q + m) \sin^2 \theta_B + f_{11,+} [1 - (\cos \theta_B - \zeta_+ \sin \theta_B)^2] - f_{11,-} [1 - (\cos \theta_B - \zeta_- \sin \theta_B)^2]}{2[f_{12,+} (\cos \theta_B - \zeta_+ \sin \theta_B) + f_{12,-} (\cos \theta_B - \zeta_- \sin \theta_B)]}. \quad (6.92)$$

where we have neglected the terms proportional to $f_{12,\pm}^2$. We can see that Eq. (6.92) is rather similar to Eq. (3.61). Since

$$\cos \theta_B - \zeta_{\pm} \sin \theta_B = \frac{\cos \theta_B \pm \beta}{1 \pm \beta \cos \theta_B} = \pm 1 \mp \frac{1}{2} \gamma^{-2} \sin^2 \theta_B (1 \pm \beta \cos \theta_B)^{-2}, \quad (6.93)$$

the last two terms in the numerator of Eq. (6.92) can be neglected compared to the first term. The denominator can be simplified to $f_{12,+} - f_{12,-} \simeq v u^{-1/2} (1 - M\beta \cos \theta_B)$, with $M \equiv 1 - 2f$. Thus, we can rewrite Eq. (6.92) as

$$\beta_p \simeq \frac{(f_{\eta} + q + m) \sin^2 \theta_B}{2v u^{-1/2} (1 - M\beta \cos \theta_B)}, \quad (6.94)$$

with

$$f_{\eta} = f_{\eta,+} + f_{\eta,-} \simeq -v\gamma^{-3} \frac{F_{\theta}}{\sin^4 \theta_B}, \quad (6.95)$$

and

$$F_{\theta} = 1 + \beta^2 \cos^2 \theta_B + 2M\beta \cos \theta_B, \quad (6.96)$$

where we have assumed $\beta \simeq 1$, $n \simeq 1$ and $\sin \theta_B \neq 0$. Similar to Sec.3.3, we write $\beta_p = \beta_0 \beta_V$, where β_0 is the polarization parameter in the absence of vacuum polarization, and β_V is the correction factor due to vacuum polarization:

$$\begin{aligned} \beta_0 &\simeq \frac{f_{\eta} \sin^2 \theta_B}{2v u^{-1/2} (1 - M\beta \cos \theta_B)} \\ &\simeq -\frac{1}{2} u^{1/2} \gamma^{-3} \frac{F_{\theta}}{\sin^2 \theta_B (1 - M\beta \cos \theta_B)}, \\ \beta_V &\simeq 1 + \frac{q + m}{f_{\eta}} \\ &\simeq 1 - \frac{q + m \sin^4 \theta_B}{v\gamma^{-3} F_{\theta}}. \end{aligned} \quad (6.97)$$

Vacuum resonance occurs at $\beta_V = 0$, corresponding to the plasma density (relative to the Goldreich-Julian density)

$$\eta_V = \frac{N_V}{N_{GJ}} = 14.15 P_1 B_{12} \nu_1^2 \gamma_3^3 \frac{\sin^4 \theta_B}{F_{\theta}} F(b). \quad (6.98)$$

Similar to Eq. (3.77) for the single stream case, the characteristic width of the resonance region is

$$\frac{\Delta N}{N_V} = 0.7157 B_{12}^{-1} \nu_1 \gamma_3^3 \frac{\sin^2 \theta_B (1 - M\beta \cos \theta_B)}{F_{\theta}}. \quad (6.99)$$

Similar to Eq. (4.85), the adiabatic condition is

$$\Gamma = \frac{2\omega H}{c} \frac{\gamma^3 \omega_p^2}{\omega_c^2 \sin^3(2\theta_m)} \frac{(1 - M\beta \cos \theta_B)^2 \sin^2 \theta_B}{F_{\theta}} \gg 1. \quad (6.100)$$

At the resonance, we have $\Gamma_V = (\nu/\nu_{\text{ad}})^3$, with

$$\nu_{\text{ad}} = 6.081 \gamma_3^{-2} F^{-1/3} \left[\frac{F_{\theta}}{(1 - M\beta \cos \theta_B) \sin^3 \theta_B} \right]^{2/3} H_6^{-1/3} \text{ GHz}, \quad (6.101)$$

Figure 8 shows the mode evolution near the vacuum resonance for different values of M 's (or f 's). For the pair plasma with $M = 0$, vacuum resonance still occurs while the resonance region is much wider compared with $M > 0$. For $-1 < M < 0$, the modes evolution behaves as the case in Fig. 6, since the linear condition is not satisfied in this parameter regime (given in the caption of the figure).

If there is a velocity spread of the electrons and positrons, for example the flat distribution given by Eq. (2.20), the equations above just need to be modified by appropriate factors similar to Eqs. (5.89) – (5.91):

$$\eta_V = \frac{N_V}{N_{GJ}} = 14.15 P_1 B_{12} \nu_1^2 \gamma_3^3 (1 - \Delta\gamma_c^2/\gamma^2)^2 \frac{\sin^4 \theta_B}{F_{\theta}} F(b). \quad (6.102)$$

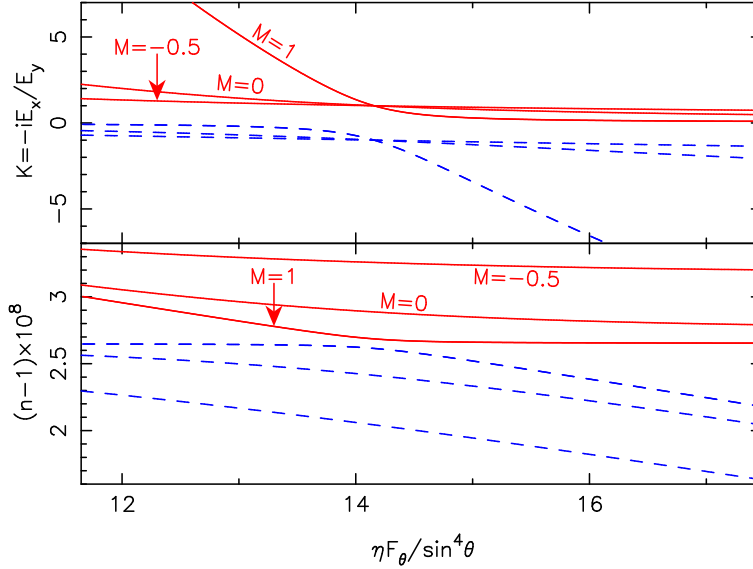


Figure 8. Same as Fig. 4, except for plasmas with two opposite streams. Note the x -axis is $\eta F_\theta / \sin^4 \theta_B$. The parameters are $B = 10^{12}$ G, $\nu = 1$ GHz, $\gamma = 10^3$, $\theta_B = 45^\circ$. For each mode, the three lines are for $M = 1 - 2f = 1, 0, -0.5$, respectively.

$$\frac{\Delta N}{N_V} = 0.7157 B_{12}^{-1} \nu_1 \gamma_3^3 (1 - \Delta \gamma_c^2 / \gamma^2)^2 \frac{\sin^2 \theta_B (1 - M \beta \cos \theta_B)}{F_\theta}. \quad (6.103)$$

$$\nu_{\text{ad}} = 6.081 \gamma_3^{-2} F(b)^{-1/3} \left[\frac{F_\theta}{(1 - M \beta \cos \theta_B) \sin^3 \theta_B} \right]^{2/3} H_6^{-1/3} \text{ GHz}. \quad (6.104)$$

7 DISCUSSION

In previous sections, we have studied the property of wave propagation in the magnetospheres of pulsars or magnetars for various plasma parameters. We have focused the vacuum resonance phenomenon, arising from the combined effects of plasma and vacuum polarization. The possible occurrence of the vacuum resonance and the related wave property depends on the plasma parameters, magnetic field and the wave frequency. The key equations are (assuming single-stream plasma):

- (i) The vacuum resonance condition, Eq. (3.73) or (3.75);
- (ii) The adiabatic condition, Eqs. (4.85 – 4.88);

In deriving the analytical expressions for the vacuum resonance, we have assumed

- (iii) The Doppler-shifted wave frequency is much less than the electron cyclotron frequency, i.e., $\omega' = \gamma \omega (1 - n \beta \cos \theta_B) \ll \omega_c$ [Eq. (3.59)];
- (iv) The plasma is weakly dispersive, i.e., $v \gamma^{-1} \ll 1$ [Eq. (3.60)].

The vacuum resonance is particularly interesting in the parameter regime such that either

- (v) the waves are linearly polarized away from the vacuum resonance due to the plasma effect [Eq. (3.69)], or
- (vi) the waves are linearly polarized away from the vacuum resonance due to the vacuum polarization [Eq. (3.70)].

Note that at the vacuum resonance, the waves are always circular polarized.

Figures 9 and 10 summarize these conditions for two different sets of parameters. In both figures, we see that when the vacuum resonance induces significant “avoided mode crossing” (cf. Figs. 4 and 5), i.e. when the resonance lies above the “Linear I” or “Linear II” line, wave evolution across the vacuum resonance is nonadiabatic. In general, this can be understood as follows. We define the cross frequency of the “Linear I” line and “Linear II” line (as well as “Vacuum Resonance” line) as ν_{cross} . We find

$$\nu_{\text{cross}} \simeq 0.58 (1 - 2f)^{-1/3} \eta^{1/3} \sin \theta_B^{2/3} P_1^{-1/3} \gamma_3^{-2} (1 - \cos \theta_B)^{-5/3} \text{ GHz}. \quad (7.105)$$

Comparing to the adiabatic frequency ν_{ad} , we have

$$\frac{\nu_{\text{cross}}}{\nu_{\text{ad}}} \simeq 0.1 (1 - 2f)^{1/3} \eta^{1/3} P_1^{-1/3} (1 - \cos \theta_B)^{1/3} F^{1/3} H_6^{1/3}. \quad (7.106)$$

For typical parameters (e.g., $f = 0 - 0.5$, $\eta = 10^2 - 10^3$, $P \sim 1$ s, $\theta = 45^\circ$, $H_6 = 1$), ν_{cross} is less than the adiabatic frequency. Adiabatic mode evolution across the vacuum resonance with appreciable mode crossing is possible for larger η and H_6 .

We now discuss possible implications of our results for various radiation processes in pulsars and magnetars. We assume a dipole magnetic field, with

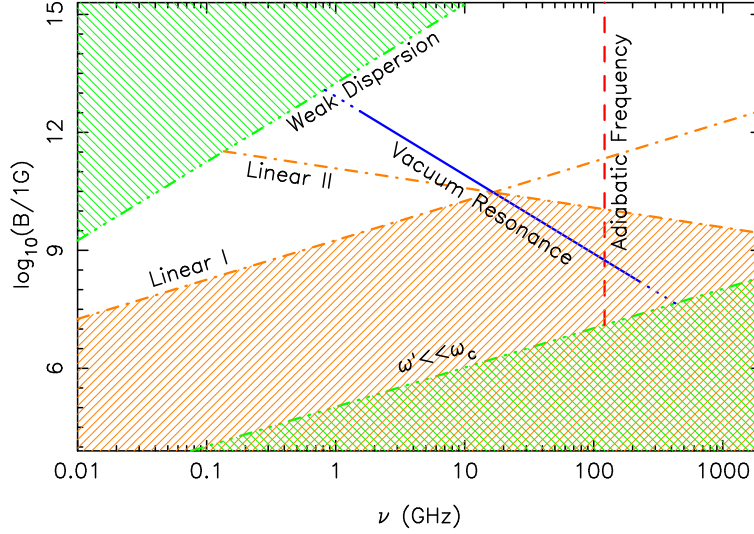


Figure 9. Vacuum resonance and wave properties in the magnetic field – frequency domain for the plasma parameters $\eta = 10$, $1 - 2f = 0.1$, $\gamma_3 = 1$, $\theta_B = 45^\circ$, $H_6 = 10$ and the NS spin period $P = 1$ s. The line labeled “Vacuum Resonance” gives the vacuum resonance condition [Eq. (3.75)], the line labeled “Adiabatic Frequency” [Eq. (4.87)] means that the adiabatic condition is satisfied to the right of the line when the wave evolves across the resonance. The line labeled “ $\omega' \ll \omega_c$ ” [Eq. (3.59)] means that the Doppler-shifted frequency is much less than the electron cyclotron frequency above the line, and the line labeled “weak dispersion” [Eq. (3.60)] means that the medium is weakly dispersive (i.e., index of refraction close to unity) below the line; Our analytical expression for the wave modes and vacuum resonance are valid in this parameter regime (below the “weak dispersion” line and above the “ $\omega' \ll \omega_c$ ” line). Above the “Linear I” line [Eq. (3.69)] or the “Linear II” line [Eq. (3.70)], the wave modes are linearly polarized except near the vacuum resonance.

$$B \approx B_* \left(\frac{R_*}{r} \right)^3, \quad (7.107)$$

where B_* is the surface magnetic field and R_* the radius of the NS star. Substituting equation (7.107) into equation (3.75), we obtain the location of vacuum resonance (assuming constant η and γ)

$$\frac{r_V}{R_*} \simeq 0.5 \left(\frac{\nu}{1 \text{ GHz}} \right)^{2/3} X \left(\frac{B_*}{10^{12} \text{ G}} \right)^{1/3} \left(\frac{\gamma}{10^3} \right) \left(\frac{\eta}{10^2} \right)^{-1/3} \left(\frac{P}{1 \text{ s}} \right)^{1/3} F^{1/3} (1 - \beta \cos \theta_B)^{2/3}. \quad (7.108)$$

Since the dispersion due to vacuum polarization is of order $q + m \propto F(b)B^2 \propto r^{-6}$, while the plasma effect is measured by $\sim v\gamma^{-3} \propto N\gamma^{-3} \propto \eta B\gamma^{-3} \propto \eta\gamma^{-3}r^{-3}$, if $\eta\gamma^{-3}$ does not vary rapidly, we find that for a given photon frequency ν , the wave dispersion is dominated by the vacuum effect for $r \lesssim r_V$ and by the plasma effect for $r \gtrsim r_V$.

First consider the radio emission from the open field line region of a pulsar. The emission angle relative the local magnetic field line is $\theta_B \sim 1/\gamma$, so that $1 - \beta \cos \theta_B \simeq \gamma^{-2}$. This would imply $r_V/R_* \ll 1$, even for $B_* \sim 10^{15}$ G and for high frequencies (e.g. $\nu = 20$ GHz). Along the ray trajectory, the angle θ_B increases. In the small angle approximation ($\theta_B \ll 1$), we have

$$\theta_B \approx \frac{3}{4} \sqrt{\frac{r_{\text{em}}}{R_*}} \theta_0 \left(1 - \frac{r_{\text{em}}}{r} \right), \quad (7.109)$$

where r_{em} is the radius of the emission point, and θ_0 is the polar angle at the stellar surface of the emission field line. Thus θ_B increases from 0 (at $r = r_{\text{em}}$) to $(3/4)(r_{\text{em}}/R_*)\theta_0$. As an example, for $r_{\text{em}} = 2R_*$ and $\theta_0 \sim \sqrt{R_*/R_{\text{LC}}} \simeq 0.0145P_1^{-1/2}$, equation (7.109) implies $\theta_B \lesssim 0.015P_1^{-1/2}$. From Eq. (7.108), we find

$$\frac{r_V}{R_*} \lesssim 0.1 \left(\frac{\nu}{20 \text{ GHz}} \right)^{2/3} \left(\frac{B_*}{10^{15} \text{ G}} \right)^{1/3} \left(\frac{\gamma}{10^3} \right)^{-1/3} \left(\frac{\eta}{10^2} \right)^{-1/3} \left(\frac{P}{1 \text{ s}} \right)^{-1/3} F^{1/3}. \quad (7.110)$$

This means that for radio emission along open, dipole field lines, plasma effects always dominate the property of wave propagation and vacuum resonance will not occur.

Radio emission may also come from the large-curvature magnetic field structure (e.g., field lines with curvature radius $\sim R_*$). In this case, even if $\theta_B \ll 1$ at emission, it will become significantly large ($\sim 45^\circ$) after the wave propagates a short distance of order R_* . Thus, according to Eq. (7.108), vacuum resonance can occur for sufficiently high frequencies and strong surface magnetic fields. This could be the case with the high-frequency radio emission from the transient AXP XTE J1810-197 (Camilo et al. 2006).

Finally, optical/IR radiation emitted from the neutron star surface or near vicinity may experience the vacuum resonance while propagating through the magnetosphere. The polarization of such radiation may probe the physical conditions of the magnetosphere.

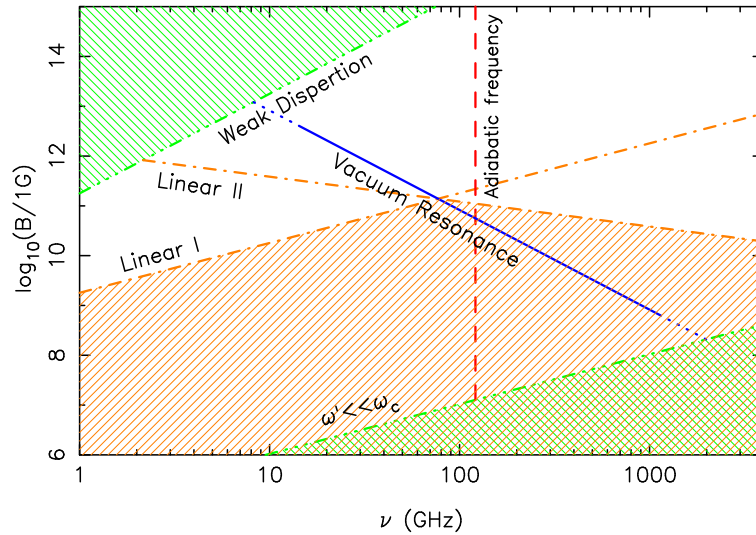


Figure 10. Similar to Fig. 9, except with different parameters: $\eta = 1000$, $1 - 2f = 0.1$, $\gamma_3 = 1$, $\theta_B = 45^\circ$, $H_6 = 10$, $P = 1$ s.

ACKNOWLEDGMENTS

We thank Qinghuan Luo for useful comment on an earlier draft of this paper. This work is supported by National Natural Science Foundation of China (10328305, 10473015 and 10521001). D.L. has also been supported in part by NSF grant AST 0307252 and NASA grant NAG 5-12034. C.W. thanks the Astronomy Department at Cornell and D.L. thanks NAOC (Beijing) for hospitality during the course of the work.

REFERENCES

- Adler, S. L. 1971, *Ann. Phys.*, 67, 599
Arons, J. & Barnard, J. J. 1986, *ApJ*, 302, 120
Asseo, E. & Riazuelo, A. 2000, *MNRAS*, 318, 983
Barnard, J. J. 1986, *ApJ*, 303, 280
Barnard, J. J. & Arons, J. 1986, *ApJ*, 302, 138
Beloborodov, A. M. & Thompson, C. 2006, astro-ph/0602417
Blaskiewicz, M., Cordes, J. M., & Wasserman, I. 1991, *ApJ*, 370, 643
Camilo, F. et al. 2006, *Nature*, 442, 892
Cheng, A. F. & Ruderman, M. A., 1979, *ApJ*, 229, 348
Daugherty, J. K. & Harding, A. K. 1982, *ApJ*, 252, 337
Gnedin, Yu. N., Pavlov, G. G., & Shibano, Yu. A. 1978, *Sov. Astron. Lett.*, 4, 117
Haberl, F. 2005, in 5 years of Science with XMM-Newton, MPE Report 288, 3944 (astro-ph/0510480)
Haberl, F., Motch, C., & Zavlin, V. E. et al. 2004, *A&A*, 424, 635
Han, J. L., Manchester, R. N., Xu, R. X., & Qiao, G. J. 1998, *MNRAS*, 300, 373
Heisenberg, W. & Euler, H. 1936, *Z. Phys.*, 98, 714
Heyl, J. S. & Hernquist, L. 1997, *Phys. Rev. D*, 55, 2449
Hibschman, J. A. & Arons, J. 2001, *ApJ*, 554, 624
Ho, W. C. G. & Lai, D. 2003, *MNRAS*, 338, 233
Kaplan, D. L., Kulkarni, S. R., & van Kerkwijk, M. H. 2003, *ApJ*, 588, 33
Kargaltsev, O. Y., Pavlov, G. G., Zavlin, V. E., & Romani, R. W. 2005, *ApJ*, 625, 307
Krall N. A. & Trivelpiece A. W. 1986, *Principles of Plasma Physics*. San Francisco Press
Kramer, M., Xilouris, K. M., Jessner, A., Lorimer, D. R., Wielebinski, R., & Lyne, A. G., 1997, *A&A*, 322, 846
Kunzl, T., Lesch, H., Jessner, A. & von Hoensbroech, A. 1998, *ApJ*, 505, 139
Lai, D. & Ho, W. C. G. 2002, *ApJ*, 566, 373
Lai, D. & Ho, W. C. G. 2003a, *ApJ*, 588, 962
Lai, D. & Ho, W. C. G. 2003b, *PhRvL*, 91, 1101L
Lyubarskii, Y. E. & Petrova, S. A. 1998, *A&A*, 333, 181
Lyutikov, M. 1998, *MNRAS*, 293, 447

- Melrose, D. B. 1973, *Plasma Physics*, 15, 99
- Melrose, D. B., Gedalin, M. E., Kennett, M. P., & Fletcher, C. S. 1999, *Journal of Plasma Physics* 62, 233
- Melrose, D. B. & Luo, Q. 2004, *MNRAS*, 352, 915
- Melrose, D. B. & Stoneham, R. J. 1977, *PASAu*, 3, 120
- Mészáros, P. & Ventura, J. 1979, *Phys. Rev. D*, 19, 3565
- Mignani, R. P. et al. 2006, astro-ph/0608025
- Mignani, R. P., de Luca, A., & Caraveo, P. A. 2004, in “Young Neutron Stars and Their Environments”, Proc. IAU Symp.218, Editors Camilo, F., Gaensler, B.M., ASP, p.391
- Petrova, L. I. 2006, *MNRAS*, 366, 1539
- Potekhin, A. Y., Lai, D., Chabrier, G. & Ho, W. C. G. 2004, *ApJ*, 612, 1034
- Radhakrishnan, V. & Rankin, Joanna M. 1990, *ApJ*, 352, 258
- Ruderman, M. 2003, astro-ph/0310777
- Schubert, C. 2001, in “Quantum Electrodynamics and Physics of the Vacuum”, Edited by Giovanni Cantatore, AIPC, V 564, p.28
- Stinebring, D. R., Cordes, J. M., Rankin, J. M., Weisberg, J. M., & Boriakoff, V. 1984a, *ApJS*, 55, 247
- Stinebring, D. R., Cordes, J. M., Weisberg, J. M., Rankin, J. M., & Boriakoff, V. 1984b, *ApJS*, 55, 279
- Thompson, C., Lyutikov, M., & Kulkarni, S. R. 2002, *ApJ*, 574, 332
- Tsytovich, V. N. & Kaplan, S. A. 1972, *Astrofizika*, 8, 441 (English transl. in *Astrophysics*, 8, 260 [1972])
- van Adelsberg, M. & Lai, D. 2006, *MNRAS*, 373, 1495
- van Kerkwijk, M. H. & Kaplan, D. L. 2006, astro-ph/0607320
- Wang, F. Y.-H., Ruderman, M., Halpern, J. P., & Zhu, T. 1998, *ApJ*, 498, 373
- You, X. P. & Han, J. L. 2006, *ChJAA*, 2, 237